Hindawi
Mathematical Problems in Engineering
Volume 2019, Article ID 4241363, 9 pages
https://doi.org/10.1155/2019/4241363

Research Article

Quasistatic Nonlinear Analysis of a Drill Pipe in Subsea Xmas Tree Installation

Haozhi Qin, Jian Liu, Wensheng Xiao, and Bingxiang Wang

College of Mechanical and Electronic Engineering, China University of Petroleum (East China), Qingdao, Shandong 266580, China

Correspondence should be addressed to Wensheng Xiao; xiaowenshengwupc@163.com

Received 13 October 2018; Revised 3 December 2018; Accepted 24 December 2018; Published 6 January 2019

Academic Editor: Roberto G. Citarella

To analyse the stress and deformation of a drill pipe during the lowering of a subsea Xmas tree, a mechanical analytical model and equation were established based on Euler-Bernoulli beam theory. The wave phase is selected as one of the variable parameters for analysis of the deformation and stress of the drill pipe. The research results indicate that the maximum response occurs at 0 radians in the scope of 0 to 2π, and the quasistatic nonlinear analysis is analysed at 0. In addition, Orcaflex software is applied for simulation, and the simulation results are compared with the results from proposed method, which demonstrate the model and the method accuracy. Factors that affect the installation process are discussed, such as current velocity, wave height, pipe size, and towing speed. The results show that all factors have remarkable effects on stress and deformation and that the wave height has a lesser effect on the deformation of the drill pipe. The viable towing speed is chosen by discussing the total stress of the drill pipe with various towing speeds and is notably useful for installation in the real sea state.

1. Introduction

With the rapid development and exploitation of offshore oil and gas from shallow to deep water regions, the subsea Xmas tree (hereafter referred to as the tree) is a key piece of equipment in the subsea production system and is widely used in deep water [1]. From shallow to deep water, the cost of the underwater equipment has not significantly increased, but the installation cost and installation risk have risen rapidly due to the complex combination of wave and current [2]. Therefore, it is necessary to analyse the motion characteristics for installation of the tree, which is important for higher safety reliability in subsea conditions. Three methods are available for installation of the tree: winch, conventional completion riser, and drill pipe. The conventional procedure with drill pipes is still widely used because this method sharply decreases the running time. In addition, the cost of using drill pipes, including maintenance costs, is quite low compared with those of the riser and winch [2, 3]. Therefore, in this paper, we choose installation of the tree lowered by a drill pipe (hereafter referred to as the pipe) as the research object.

In recent years, scholars have performed many studies on the installation of the tree, most of which consist of engineering application reports and installation process or method studies, but mechanics analyses have not been frequently reported. Moreira [3] introduced an engineering project in the Roncador field in the northern area of the Campos Basin, and subsea trees were installed via drill pipe at a water depth of 1800 m. Moreira suggests that the method with a drill pipe is better than the method with risers in lowering of subsea trees in deep water. Rober [4] documented the results of West African installation data analysis and showed the complete process of tree installation, including equipment, installation process, and working hours.

The installation of the tree can refer to the installation of the marine drilling riser or the hang-off marine drilling riser during emergency evacuation. Both the pipe and marine drilling riser can be viewed as slender marine structures, and many scholars have studied the mechanical behaviours of a slender structure in deep water. Patel and Jesudasen [5] presented a theoretical and experimental investigation of the lateral dynamics of free-hanging marine drilling risers. Gosse and Barsdale [6] established a mathematical model of the riser under working conditions and derived the vibration equation. Sheng et al. [7] discussed the riser in the context of hang-off modes under typhoon conditions in

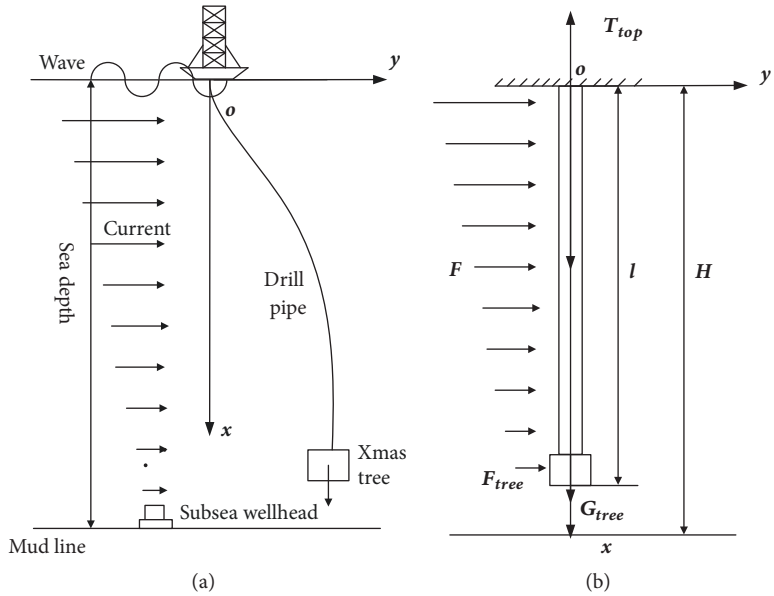

Figure 1: Schematic diagram and mechanical analysis model for the subsea Xmas tree installation process. (a) Schematic diagram. (b) mechanical analysis model.

the South China Sea in which the soft/hard riser hang-off configurations for storm events were assessed. Hu et al. [8] analysed the dynamic characteristics of the riser in the time domain throughout the entire installation operation (from the vessel to the wellhead) and took the launch velocity as a variable parameter. This research supplied a new method for study of the variable-length riser. Considering the water depth, riser size, BOP weights, and weather conditions, Wang et al. [9, 10] analysed the static behaviour and lateral vibration of the riser during the installation process.

Many scholars have also studied modelling methods for a drilling riser. The finite element method is the most common approach to modelling the drilling riser in these studies [11–13]. Gosse and Barksdale [14] established a mathematical model to analyse the marine riser, and the differential equation was solved using the finite difference approximation. Raman-Nair and Baddour [15] formulated the equation of 3D motion of a marine riser using Kane's formalism, where the riser is modelled using lumped masses connected by extensional and rotational springs, including structural damping. Wu et al. [16] applied the Newmark-β method and Newton-Raphson iteration method to obtain the numerical solution of the dynamical model for the hang-off drilling riser. Considering the internal solitary wave and vessel motion, Fan et al. [17] conducted dynamic analysis of a hang-off drilling riser, constructed a dynamic model based on the Euler-Bernoulli theory, and solved the structural governing equation using the Wilson-θ method. Xu and Wang [18] modelled the drilling riser using the finite segment method and reported a lineation iteration scheme to solve the nonlinear equations.

Many articles also use software to simulate the slender marine structures and calculate their mechanical properties and deformation. Qi [19] calculated the evacuation speed range of a hard hang-off drilling riser due to a typhoon using Orcaflex. Bai et al. [20] performed 3D mechanical research on a manifold installation by drill pipe in deep water that considered the vessel's RAO, wave loads, and lowering velocity. This theoretical method was proved to be accurate using a numerical simulation based on Orcaflex software. Dai et al.[21] simulated the dynamic characteristics of the drilling riser under hang-off working conditions using ABAQUS.

In previous research, authors introduced various methods to calculate the response characteristics related to installation of a long slender structure in ultra-deep water. However, in the existing research, parameters such as wave phase angle and vessel towing speed (applied to drag the tree in place) were normally neglected, especially in static analysis, and the influence of wave phase angle was ignored, resulting in a large deviation from the real situation.

In this paper, installation of the tree with a pipe is investigated under the combination of wave and current. The influence of phase angle on the installation process is studied in the range of 0-2π. The phase angle leading to the largest response characteristic in the process is identified. The angle used to perform quasistatic analysis on the pipe is investigated for different values of current velocity, wave height, and drill pipe size. The accuracy and effectiveness of the proposed numerical analysis method can be proved by comparison with the simulation run using Orcaflex software.

2. Mathematical Model

2.1. Model Analysis. In the process of tree installation, the top of the pipe is rigidly linked to the installation vessel by the lowering device [2], and the bottom is connected to the tree as a lumped mass. The pipe is subjected to the axial tension force generated by the vessel, the self-weight, the tree weight, and the lateral force generated by the combined action of wave and current, as shown in Figure 1(a).

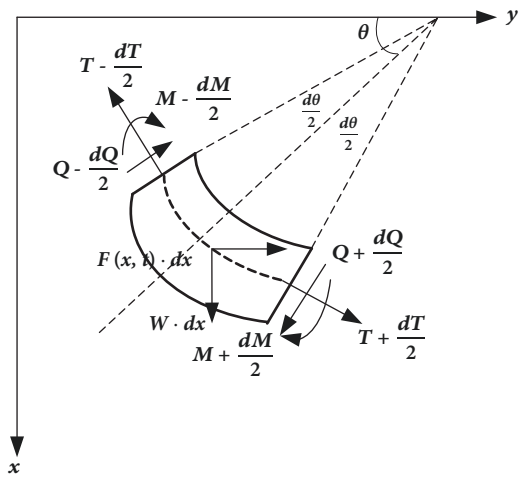

Figure 2: The pipe micro body analysis model.

In order to perform convenient calculation and formula derivation, the following assumptions are applied during equation deduction:

(i) The material of the drill pipe is linearly elastic, isotropous, and homogeneous.

(ii) The pipe out diameter is regarded as constant cross-section.

(iii) The mechanical characters of the pipe are under large deformation with small strain.

(iv) The pipe is with variable axial tension and variable hydrodynamic force.

(v) The pipe top is connected with the vessel and is regarded as a fixed end without displacement.

The installation model can be simplified as a cantilever beam with a lumped mass located in the vertical plane. The coordinate system is established on the free surface of the sea, and the positive direction of the x-axis points vertically to the bottom of the sea, and the positive direction of the y-axis is the same as the flow direction, as shown in Figure 1(b).

In order to obtain the pipe differential equation during installation, a micro body with length dx is cut off at the water depth x from the sea surface, and the force analysis of the micro body is shown in Figure 2.

Considering the effective axial tension force and the combined hydraulic load, the fourth-order partial differential equation is applied as the pipe governing equation:

$$EI\frac{\partial^4 y}{\partial x^4} - T(x)\frac{\partial^2 y}{\partial x^2} + W\frac{\partial y}{\partial x} = F(x,t) \tag{1}$$

In (1), t is the time; x is the coordinate measured along the axis of the pipe; $y(x,t)$ is the transverse deflection of the beam axis; E is the modulus of elasticity; I is the area moment of inertia; $T(x)$ is the axial tension force of the beam; W is the submerged weight of the pipe per unit length; and $F(x, t)$ is the combined hydraulic load distribution per unit of length along the x-axis.

Eq. (2) presents the boundary conditions of the pipe at x=0 and x=l:

$$\begin{aligned} y|_{x=0} &= 0; \\ \theta|_{x=0} &= 0 \\ Q|_{x=l} &= F_{tree}; \\ M|_{x=l} &= 0 \end{aligned} \tag{2}$$

where l is the length between the pipe fixed end and free end; θ is the deflection angle of the pipe relative to the x-axis; Q is the shearing force acting on the pipe; F_{tree} can be treated as the lateral force applied to the tree; and M is the bending moment.

2.2. Load Analysis. The tree is suspended by the pipe. Suppose that the tension force of the pipe is $T(x)$, the submerged weight of the tree is G_{tree}, and the tension force on the pipe section can be represented by the following:

$$\begin{aligned} W &= \frac{1}{4}\pi g(\rho_s - \rho_w)\left(D^2 - d^2\right) \\ T(x) &= G_{tree} + \int_x^l W dx \end{aligned} \tag{3}$$

where x is the distance from the section to the top of the pipe; ρ_s is the density of the pipe; ρ_w is the density of seawater; W is the submerged weight of the pipe per unit length; and D and d are the outer and inner diameters of the pipe, respectively.

The lateral force on the pipe is mainly generated by the sea waves and ocean current. The combined wave and current force can be accepted according to the Morison equation [14]:

$$\begin{aligned} F(x,t) = {} & \frac{1}{2}C_D\rho_w D(u_w + u_c)\left|u_w + u_c\right| \\ & + \frac{1}{4}C_m\rho_w\pi D^2 a_w \end{aligned} \tag{4}$$

where C_D is the drag force coefficient; C_m is the inertia force coefficient; u_w is the horizontal velocity of the fluid particle; u_c is the current speed; and a_w=du_w/dt is the horizontal acceleration of fluid particle.

According to the Ekman transport theory, the velocity of the deep ocean current can be calculated by the following[22]:

$$u_c = \begin{cases} V_{CW}\left(\dfrac{d_0 - x}{d_0}\right) + V_d\left(\dfrac{H - x}{H}\right)^{1/7} & x \leqslant d_0 \\ V_d\left(\dfrac{H - x}{H}\right)^{1/7} & x > d_0 \end{cases} \tag{5}$$

where V_W is the observed wind speed; V_{CW} is the wind current velocity amplitude; d_0=50m, which is recommended

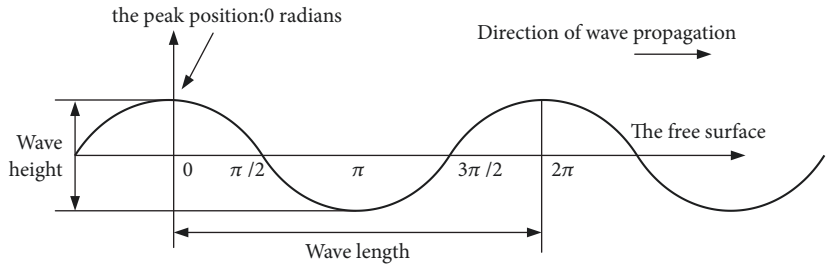

Figure 3: Definition of wave phase angle.

by DNV-RP-C205, is reference depth for wind-generated current; V_d is the tidal velocity; H is the depth of the sea; and φ is the latitude of the location.

In this paper, both the horizontal velocity and the acceleration of the fluid particle can be described with linear wave theory:

$$u_w = \frac{\pi H'}{T} \frac{\cosh k(H-x)}{\cosh kH} \cos(ky - \omega t)$$
$$a_w = \frac{2\pi^2 H'}{T^2} \frac{\cosh k(H-x)}{\cosh kH} \sin(ky - \omega t) \quad (6)$$

where H' is the wave height; H is the sea depth; T is the wave period; k is the wave number; ω is the angular frequency; and the wave phase is $\alpha = ky - \omega t$.

According to (4) and (6), the wave phase angle can affect the speed and acceleration of the wave, and, consequently, the wave load on the pipe also changes with the wave phase. As shown in Figure 3, suppose that the phase angle of the peak position is 0 radians at time t which equals 0. In the range of 0 to 2π, the interval is $\pi/180$ and the effect of the hydrodynamic force on the pipe is calculated to obtain the maximum response of the installation process in quasistatic conditions.

3. Model Solution

Because of the influences of many factors in (1) and (2), the stress state of the pipe is so complicated that it is difficult to directly obtain the analytical solution. To solve this problem conveniently, the finite difference method is generally applied. As shown in Figure 4, the pipe is modelled as a hollow cylinder beam divided into n segments, and the length of each section is h. The first node is located on the top of the pipe and denoted by No. 1, and the last node is located on the tree and is denoted by No. (n+1). The mass of each segment is lumped at the end, except for No. (n+1), which includes the mass of the tree; i.e., the tree is merged into the last point of the pipe.

Because (1) is a fourth-order partial differential equation, according to the finite difference method, the derivative is replaced by the difference quotient term, as shown in

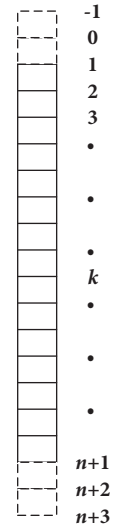

Figure 4: Schematic diagram of pipe discretization.

$$\left(\frac{dy}{dx}\right)_k = \frac{y_{k+1} - y_{k-1}}{2h} + o(h)$$
$$\left(\frac{d^2y}{dx^2}\right)_k = \frac{y_{k+1} - 2y_k + y_{k-1}}{h^2} + o\left(h^2\right)$$
$$\left(\frac{d^3y}{dx^3}\right)_k = \frac{y_{n+3} - 2y_{n+2} + y_n - y_{n-1}}{h^3} + o\left(h^3\right) \quad (7)$$
$$\left(\frac{d^4y}{dx^4}\right)_k = \frac{y_{k+2} - 4y_{k+1} + 6y_k - 4y_{k-1} + y_{k-2}}{h^4} + o\left(h^4\right)$$

where x_k is the coordinate of the No. (k) node on the x-axis and y_k is the deflection of the No. (k) node.

To calculate the parameters of the points at both ends of the pipe, we need to assume the continuation point of the two ends and obtain the nodes of No. -1, No. 0, No. (n+2), and No. (n+3). Therefore, there are n+5 nodes in total.

The pipe discretization control differential equation can be deduced by substituting (7) and (3) into (1), as shown in

$$\frac{EI}{h^4}y_{k+2} - \left(\frac{4EI}{h^4} + \frac{T}{h^2} - \frac{W}{2h}\right)y_{k+1} + \left(\frac{6EI}{h^4} + \frac{2T}{h^2}\right)y_k - \left(\frac{4EI}{h^4} + \frac{T}{h^2} + \frac{W}{2h}\right)y_{k-1} + \frac{EI}{h^4}y_{k-2} = F(k,t) \quad (1 \leqslant k \leqslant n+1) \tag{8}$$

After discretization, there are (n+5) nodes, meaning that there are a total of (n+5) unknown parameters (y_{-1}, y_0, …, y_{n+3}). In (8), the value of the parameter k ranges from 1 to n+1 for a total of (n+1) equations. Therefore, four boundary condition equations are required. According to the analysis model of tree installation, the four boundary condition equations are given as follows: the deflection of the pipe top (node No. 1) is 0, the deflection angle of the pipe top (node No. 1) is 0, the shear force on the pipe end (node No. n+1) is the sum of the lateral fluid loads that act on the pipe and the tree, and the bending moment of the pipe end (node No. n+1) is 0. Thus the discretization forms of boundary conditions can be expressed as follows:

$$\begin{aligned} y_1 &= 0 \\ y_2 - y_1 &= 0 \\ y_{n+2} - 2y_{n+1} + y_n &= 0 \\ \frac{y_{n+3} - 2y_{n+2} + y_n - y_{n-1}}{h^3} &= \frac{F_{tree}}{EI} \end{aligned} \tag{9}$$

Considering (8) and (9), there are (n+5) equations, and, therefore, the deflection of (n+5) nodes can be solved. The matrix form of the equation is given as shown in

$$[A] \cdot [Y] = [b] \tag{10}$$

where $[A]$ is the coefficient matrix, $[Y] = [y_{-1}\ y_0\ y_1\ \cdots\ y_{n+1}\ y_{n+2}\ y_{n+3}]^T$ is the matrix of the pipe deflection at each discrete node (which is an (n+5) order square matrix), and $[b] = [F(x_1)\ F(x_2)\ \cdots\ F(x_{n+1})\ 0\ 0\ 0\ F_{tree}/EI]^T$ is the matrix of known parameters (which is an (n+5) order column matrix). After (10) is solved, the matrix $[Y]$ can be obtained, and thus the bending moment at each discrete node is described by the equation

$$M(x) = EI\frac{d^2y}{dx^2} \tag{11}$$

4. Example Calculation and Analysis

4.1. Example. Taking an actual subsea Xmas tree installation process as an example, the known parameters are listed in Table 1.

4.2. Wave Phase Angle Analysis. According to the theory of material mechanics, the maximum stress of the curved beam appears on the outer wall, where one side is under compressive stress and the other side is under tensile stress. The pipe is subjected to both axial tension force and lateral force during the tree installation process, and, therefore, the maximum stress is tensile stress on the outer wall of the pipe. Figure 5 shows the relationship between the maximum stress on the pipe and the wave phase angle in this calculation case. The maximum stress of the pipe is 594.6 MPa, which occurs when the angle is $\pi/18$. When the phase angle is$19\pi/18$, the minimum stress value is 581.1MPa. As observed from Figure 6, the displacement of the pipe end changes with the various phase angles. The maximum displacement occurs at the angle of $\pi/18$, and a minimum offset occurs when the phase angle is $19\pi/18$.

Both the displacement of the tree and the total stress of the pipe reach the maximum value at the angle of $\pi/18$. That

Table 1: Known parameters.

Property	Value
Sea depth (H)/m	1500
Density of sea water (ρw)/kg/m^3	1025
Wave height (H')/m	6.5
Wave period (T)/s	8.5
Surface wind-generated current velocity (V_{CW})/m/s	1
Tidal velocity (Vd) /m/s	1
Latitude of the location (φ)/rad/s	$\pi/4$
Density of drill pipe (ρs)/kg/m^3	7850
Elastic modulus of steel (E)/GPa	206
Outside diameter (D)/mm	127
Thickness of pipe (δ)/mm	9.19
Drag force coefficient (Cd)	1.2
Inertia force coefficient (Cm)	1.6
Weight of tree (G_{tree})/kN	500
Drainage volume of tree (V)/m^3	15.3
Drag area of tree (S)/ m^2	10
Number of drill pipe segments (n)	1500

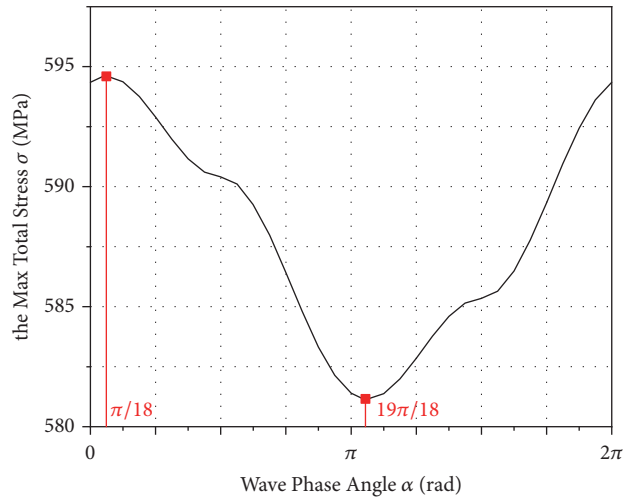

Figure 5: Stress with changing angle.

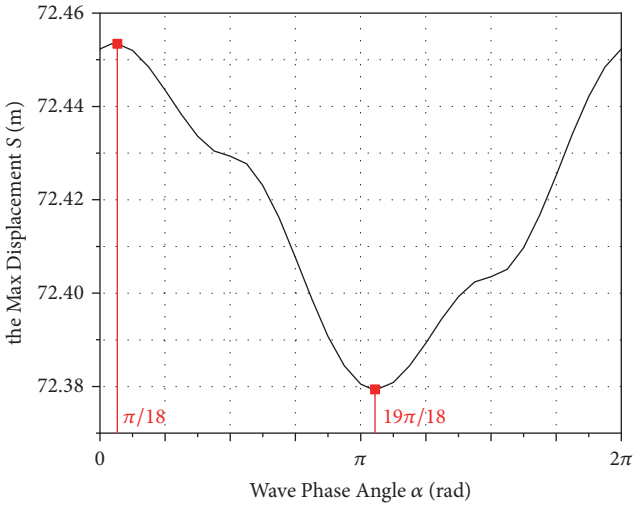

FIGURE 6: Displacement of pipe end at different phase angles.

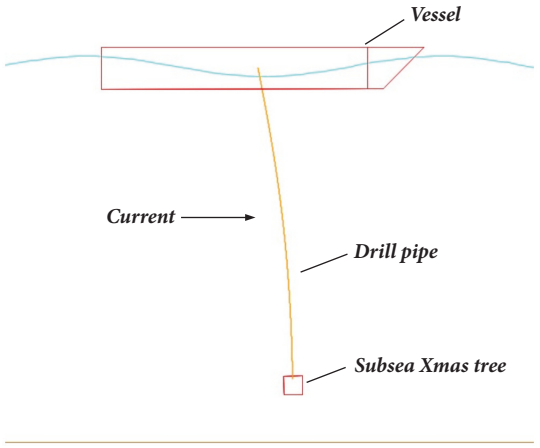

FIGURE 7: Sketch of Orcaflex model.

being said, the installation process has a maximum response at the $\pi/18$. Therefore, the phase angle should be taken as $\pi/18$ during quasistatic analysis of the installation process.

4.3. Orcaflex Simulation Comparison. In this section, as shown in Figure 7, a finite element model using the Orcaflex software is employed to analyse the dynamic behaviour of the pipe during the installation process in time domain. The current velocity profile is obtained by (5), and the type of wave is Airy model. The pipe is modelled by line element with same geometrical features. In practical engineering, a Xmas tree is an assembly of valves, and a 6D spar buoy is selected to model the tree to simplify the physical model. Meanwhile, a vessel element is used to model the semisubmersible platform.

As shown in Figure 8, because of the combined action of the lateral and axial forces, the lateral deformation of the pipe is obviously increased at the beginning and is few changes at the bottom. In this case, using the proposed method, the displacement of tree is 72.4 m; i.e., when the tree reaches the seabed, it is located 72.4 m away from the wellhead.

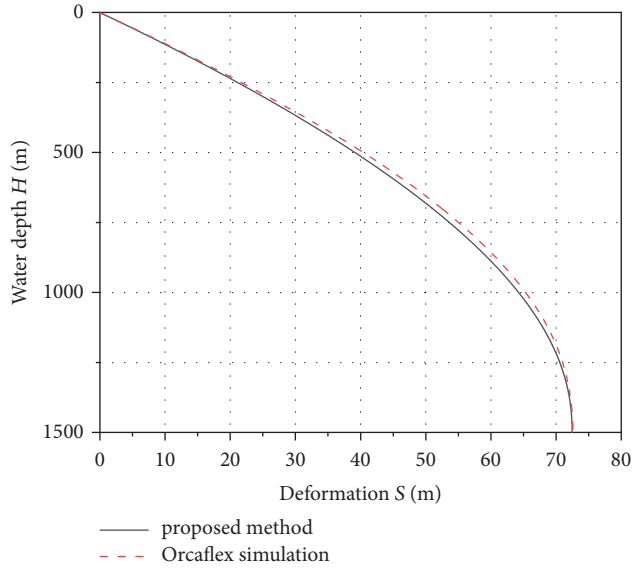

FIGURE 8: Pipe deformation when the tree falls to the mud line.

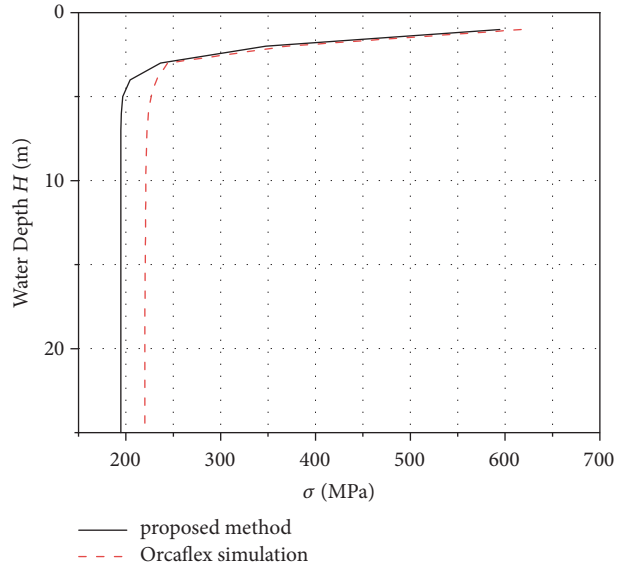

FIGURE 9: Total stress of the pipe distribution with depth.

According to the Orcaflex software simulation, the lateral displacement of the tree is 72.6 m. Error of 0.3% is noted between the two results.

According to Figure 9, the maximum tensile stress of the pipe is located on the joint of the pipe with the vessel. Almost no difference is found between the proposed method and Orcaflex simulation for the problem of the maximum tensile stress of the pipe. The maximum tensile stress obtained by proposed method is 594.6MPa, and, using Orcaflex software, the maximum tensile stress is 617 MPa. For the two methods, the error is only 3.8%. However, for the stress at the other positions of the pipe, the simulation results are larger than the theoretical calculation values because the coupled relations

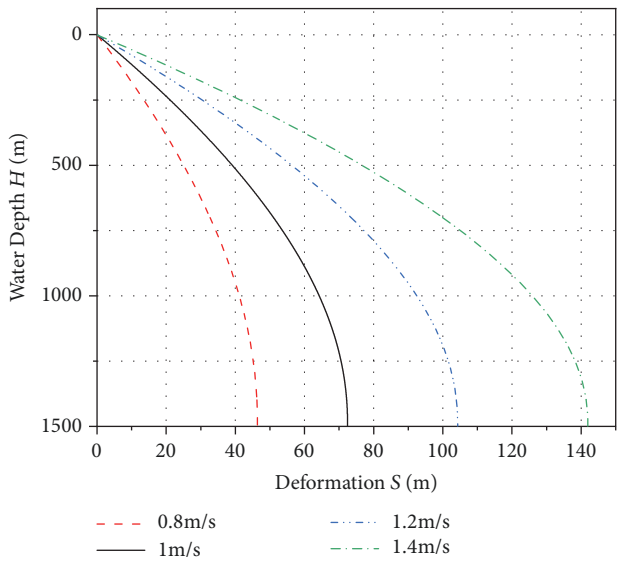

Figure 10: Variations of pipe deflection with sea surface tide velocity.

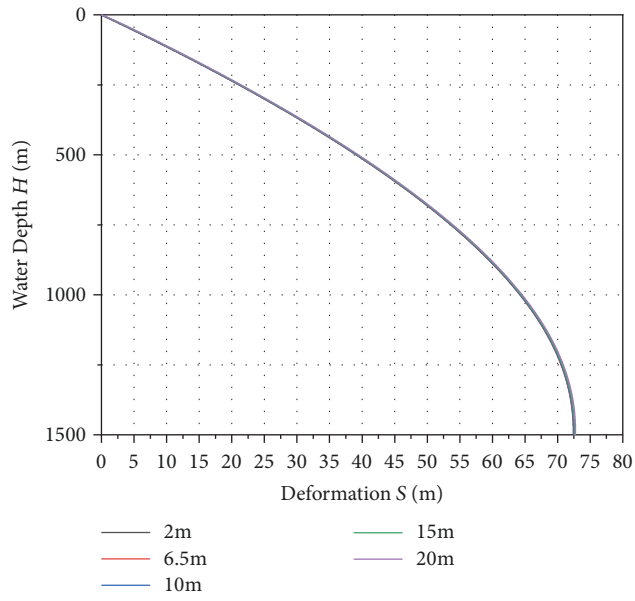

Figure 11: Variations of pipe deflection with wave height.

between longitudinal vibration, lateral vibration, and vessel motion are not considered in the proposed method.

4.4. Analysis of Influencing Factors

4.4.1. Sea Surface Tide Velocity. The variation of the pipe deflection with sea surface tide velocity (which ranges from 0.8 m/s to 1.4 m/s) for four different speeds is shown in Figure 10. The tidal current speed has a great influence on the deformation of the pipe. As the tidal current speed increases, the displacement of the tree and the maximum deformation of the pipe increase significantly. Therefore, the tidal current velocity should be accurately measured before the tree is lowered to prevent excessive bending deformation of the pipe.

4.4.2. Wave Height. The variations of the pipe deflection and the maximum stress with five different wave heights are shown in Figures 11 and 12, respectively. The lateral offsets of the pipe at five different wave heights are minimally changed, which indicates that the wave height has a minor effect on the offset of the tree. However, the stress on the top of the pipe increases as the wave height rises.

4.4.3. Drill Pipe Size. Assuming that the other parameters are constant, the deformation and maximum stress of the pipe were examined using four common pipe sizes, as shown in Figures 13 and 14.

Figure 11 shows that both the offset of the tree and the deflection of the pipe are significantly different for different sizes of the pipe. The larger the pipe size is, the larger the drag area of the pipe will be, and the drag and inertial forces on the pipe are greater such that the deformation of the pipe is larger. At the same time, the maximum stress on the top of the pipe also significantly increases with size. Therefore, under the same sea conditions, if the strain of the pipe is available

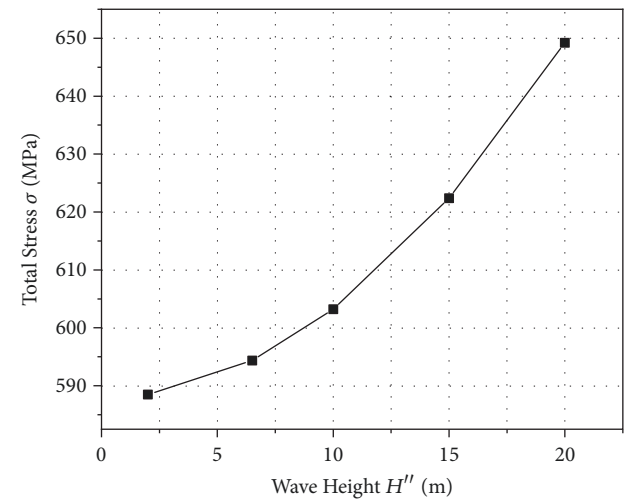

Figure 12: Variations of pipe maximum stress with wave height.

for the strength requirement, a thinner drill pipe can reduce the displacement of the tree and the tensile stress of the pipe.

4.4.4. Towing Speed. Once the tree is lowered to a position 10-20 m above the mud line, the next step is to examine the vessel motion to offset the lateral distance between the tree and the subsea wellhead. During the towing process, the pipe deformation increases. As shown in Figure 15, assuming four values of towing speed, the total stress on the pipe increases with the towing speed, and the stress at the top of the pipe increases especially sharply. If the vessel moves too rapidly, it causes yield deformation at the top of the pipe. Therefore, a reasonable towing speed should be chosen according to the real sea state before moving the vessel. In this case, the minimum yield strength is 1138MPa, and the total stress is as

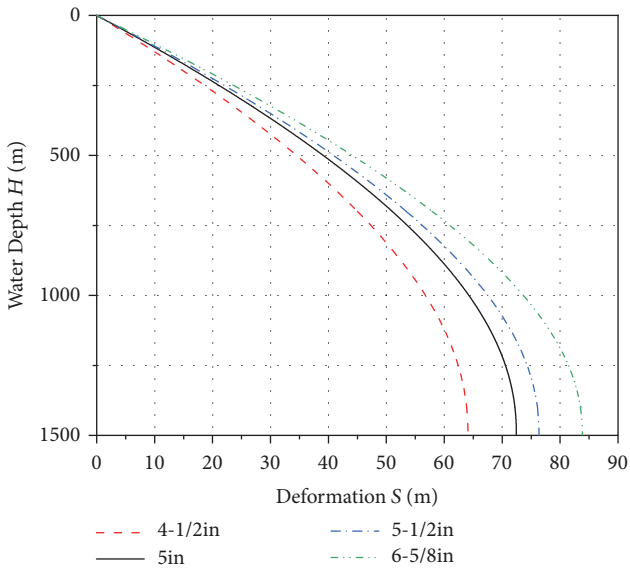

Figure 13: Variations of pipe deflation with rise size.

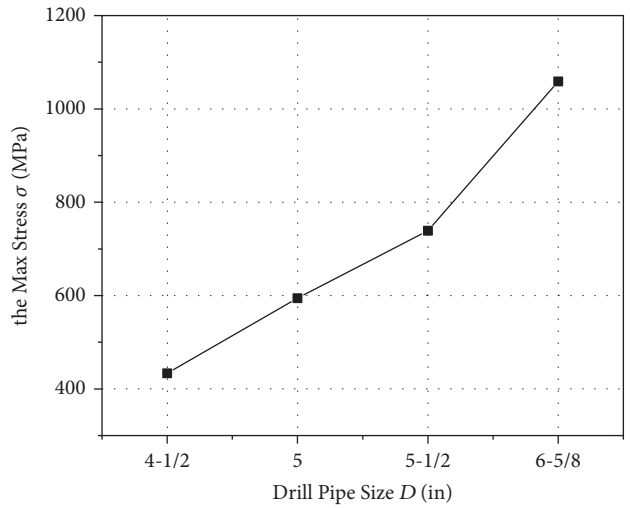

Figure 14: Variations of pipe maximum stress with rise size.

high as 1170 MPa when the towing speed is 3 knots; i.e., the movement speed of the vessel must be less than 3 knots.

5. Conclusions

This paper studies quasistatic geometric nonlinear analysis of drill pipe applied to the subsea Xmas tree installation. Several conclusions are given as follows.

(1) In order to analyse the pipe stress and deformation during the tree installation, a quasistatic analysis model and a nonlinear partial differential equation were established, and the equation was solved by using the finite difference method. In this model, the pipe was simplified as a cantilever beam with a lumped mass.

(2) In order to find out the maximal combined wave-current loads, a quasistatic analysis of the pipe was performed, and the total stress and the deformation of the pipe as

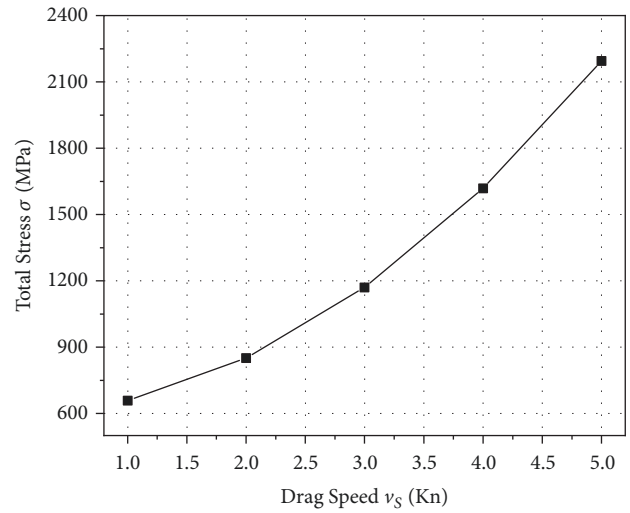

Figure 15: Variations of pipe total stress with towing speed.

the criterion for search of the maximal wave phase angle was proposed. The results indicate that the maximum total stress occurs at the zero phase angle of the wave.

(3) A finite element model using the Orcaflex software was employed to analyse the behaviour of the pipe during the installation process. Results from the proposed method and the Orcaflex simulation show the great agreement, which verifies the effectiveness of the proposed method.

(4) The effect of different factors such as sea surface tide (current) speed and wave height on the pipe deformation and total stress was discussed. The tide (current) speed is the most critical factor for the lowering process. As the water flow speed increases, the lateral offset of the tree and the maximum stress of the pipe increase sharply.

(5) Drill pipe bending deformation and stress increase with increase of sea surface tide (current) speed, wave height, the pipe size, and drag speed. Among these, the tide (current) speed is the most critical factor for the lowering process. As the water flow speed increases, the lateral offset of the tree and the maximum stress of the pipe increase sharply. Moreover, the total stress of the pipe increases significantly with the increase of the drag speed. Under a certain sea state and drill pipe size, the maximum allowable drag speed can be obtained.

Data Availability

The known parameters in Table 1 used to support the findings of this study are included within the article.

Conflicts of Interest

The authors declare that they have no conflicts of interests with respect to publication of this paper.

Acknowledgments

The authors acknowledge the Ministry of Industry and Information Technology of the PR China for support of this

study through the project "Development of Subsea Vertical Christmas Tree" under grant number (2013)420. This work was also funded by the Key Laboratory of Shandong Province Offshore Petroleum Equipment, Shandong Kerui Machinery Manufacturing Co., Ltd.

References

[1] Y. Bai and Q. Bai, *Subsea Manifolds, in: Subsea Engineering Handbook*, chapter 19, Gulf Professional Publishing, Boston, Mass, USA, 2010.

[2] Y. Wang, H. Tuo, L. Li, Y. Zhao, H. Qin, and C. An, "Dynamic simulation of installation of the subsea cluster manifold by drilling pipe in deep water based on OrcaFlex," *Journal of Petroleum Science and Engineering*, vol. 163, pp. 67–78, 2018.

[3] J. Moreira and T. Johansen, "Installation of Subsea Trees in Roncador Field, at 1800m Water Depth Using the Drill Pipe Riser," in *Proceedings of the Offshore Technology Conference*, Houston, Texas, USA, 2001.

[4] R. Voss and T. Moore, "Subsea Tree Installation, Lessons Learned on a West Africa Development," in *Proceedings of the Offshore Technology Conference, Offshore Technology Conference*, Houston, Tex, USA, 2003.

[5] M. H. Patel and A. S. Jesudasen, "Theory and model tests for the dynamic response of free hanging risers," *Journal of Sound and Vibration*, vol. 112, no. 1, pp. 149–166, 1987.

[6] C. G. Gosse and G. L. Barsdale, "The Marine Riser- A Procedure for Analysis," in *Proceedings of the Offshore Technology Conference, Offshore Technology Conference*, Houston, Tex, USA, 1969.

[7] S. Leixiang, X. Liangbin, Z. Jianliang, J. Shiquan, and L. Xunke, "Experience on Deepwater Drilling Riser about Hang-off Modes in Typhoon Condition of South China Sea," in *Proceedings of the Offshore Technology Conference Asia, Offshore Technology Conference*, Kuala Lumpur, Malaysia, 2016.

[8] Y. Hu, J. Cao, B. Yao, Z. Zeng, and L. Lian, "Dynamic behaviors of a marine riser with variable length during the installation of a subsea production tree," *Journal of Marine Science and Technology*, pp. 378–388, 2017.

[9] Y. Wang, D. Gao, and J. Fang, "Static analysis of deep-water marine riser subjected to both axial and lateral forces in its installation," *Journal of Natural Gas Science and Engineering*, vol. 19, pp. 84–90, 2014.

[10] Y. Wang, D. Gao, and J. Fang, "Study on lateral vibration analysis of marine riser in installation-via variational approach," *Journal of Natural Gas Science and Engineering*, vol. 22, pp. 523–529, 2015.

[11] O. C. Zienkiewicz and R. L. Taylor, *The Finite Element Method*, vol. 2 of *Solid Mechanics*, Butterworth-Heinemann, Oxford, UK, 5th edition, 2000.

[12] Z.-S. Chen and W.-J. Kim, "Numerical investigation of vortex shedding and vortex-induced vibration for flexible riser models," *International Journal of Naval Architecture and Ocean Engineering*, vol. 2, no. 2, pp. 112–118, 2010.

[13] G. A. Jensen, N. Säfström, T. D. Nguyen, and T. I. Fossen, "A nonlinear PDE formulation for offshore vessel pipeline installation," *Ocean Engineering*, vol. 37, no. 4, pp. 365–377, 2010.

[14] C. G. Gosse and G. Barsdale, "The Marine Riser- A Procedure for Analysis," in *Proceedings of the Offshore Technology Conference, Offshore Technology Conference*, p. 8, Houston, Tex, USA, 1969.

[15] W. Raman-Nair and R. E. Baddour, "Three-dimensional dynamics of a flexible marine riser undergoing large elastic deformations," *Multibody System Dynamics*, vol. 10, no. 4, pp. 393–423, 2003.

[16] W. Wu, J. Wang, Z. Tian et al., "Dynamical Analysis on Drilling Riser Evacuated in Hard Hang-off Mode," in *Proceedings of the The Twenty-fourth International Ocean and Polar Engineering Conference, International Society of Offshore and Polar Engineers*, Busan, Korea, 2014.

[17] H. Fan, C. Li, Z. Wang, L. Xu, Y. Wang, and X. Feng, "Dynamic analysis of a hang-off drilling riser considering internal solitary wave and vessel motion," *Journal of Natural Gas Science and Engineering*, vol. 37, pp. 512–522, 2017.

[18] X.-S. Xu and S.-W. Wang, "A flexible-segment-model-based dynamics calculation method for free hanging marine risers in re-entry," *China Ocean Engineering*, vol. 26, no. 1, pp. 139–152, 2012.

[19] M. Qi, L. Li, L. Song, Y. Cheng, D. Wang, and X. Zhang, "Configuration and Operation Optimization of Deepwater Drilling Riser Considering of Evacuation due to Typhoon," in *Proceeding of the Twenty-fifth International Ocean and Polar Engineering Conference, International Society of Offshore and Polar Engineers*, p. 5, Kona, Hawaii, USA, 2015.

[20] Y. Bai, W. Ruan, S. Yuan, X. He, and J. Fu, "3D mechanical analysis of subsea manifold installation by drill pipe in deep water," *Ships and Offshore Structures*, vol. 9, no. 3, pp. 333–343, 2014.

[21] W. Dai, F. Gao, and Y. Bai, "FEM analysis of deepwater drilling risers under the operability and hang-off working conditions," *Journal of Marine Science and Application*, vol. 8, no. 2, pp. 156–162, 2009.

[22] DNV, Recommended Practice DNV-RP-C205: Environmental Conditoins and Environmental Loads, Det Norske Veritas 2010.